# Investigation of Optical Properties and Defects Structure of Rare Earth (Sm, Gd, Ho) Doped Zinc Oxide Thin Films Prepared by Pulsed Laser Deposition

M. Novotny[a,*], P. Hruska[a,b], P. Fitl[a], E. Maresova[a,c], S. Havlova[a,c], J. Bulir[a],
L. Fekete[a], R. Yatskiv[d], M. Vrnata[c], J. Cizek[b], M.O. Liedke[e] and J. Lancok[a]

[a]Institute of Physics of the Czech Academy of Sciences, Na Slovance 2, CZ 182 21 Praha 8, Czech Republic
[b]Faculty of Mathematics and Physics, Charles University, V Holesovickach 2, CZ 180 00 Praha 8, Czech Republic
[c]University of Chemistry and Technology, Prague, Technicka 5, CZ 166 28 Praha 6, Czech Republic
[d]Institute of Photonics and Electronics of the Czech Academy of Sciences,
Chaberska 57, CZ 182 51 Praha 8, Czech Republic
[e]Helmholtz-Zentrum Dresden-Rossendorf, Institute of Radiation Physics,
Bautzner Landstr. 400, 01328 Dresden, Germany

Rare earths (RE = Sm, Gd, Ho) doped ZnO thin films were grown by pulsed laser deposition in oxygen ambient at pressure of 10 Pa on fused silica and Si(100) substrates at room temperature. A good optical quality of the films was confirmed by transmittance measurement in the visible spectral region. Photoluminescence suggested $RE^{3+}$ oxidation state as confirmed at ZnO:Sm, where local structure was inhomogeneous. ZnO:Sm film exhibited the highest electrical resistivity while ZnO:Ho the lowest. Nanocrystalline structure of the films was observed by atomic force microscopy and X-ray diffraction. Defects structure was examined by variable energy positron annihilation spectroscopy. All ZnO:RE films exhibited significantly higher values of the $S$ parameter as well as shorter positron diffusion lengths compared to ZnO monocrystal reference due to trapping of positrons at open volumes associated with grain boundaries. We observed the impact of the type of RE dopant on optical and electrotransport properties while the defect structure remained unchanged.

## 1. Introduction

In past decades a lot of efforts have been put in fabrication of high-quality zinc oxide thin films [1]. Such films of low defect concentrations can serve as a part of several optoelectronics devices (waveguides, LEDs, solar cells, and sensors) [1, 2]. The optical properties can be tuned and enhanced by doping ZnO with rare earth ($RE^+$) elements usually up to 5 at.% [3, 4]. Strong emission lines in ZnO:RE structures can be obtained in the visible and infrared spectral region [4–9].

Pulsed laser deposition (PLD) has been shown as a promising technique for the fabrication of thin films of complex structure. ZnO films prepared by PLD exhibit typically oxygen deficiency leading to an enhanced concentration of oxygen vacancies [10, 11]. Deposition in an oxygen enriched atmosphere can eliminate this problem and eventually create Zn vacancies. Positron annihilation spectroscopy (PAS) has been successfully employed in defects studies of ZnO bulks [12, 13] and ZnO films grown by PLD [11, 14, 15]. PAS has not been utilized yet in defect studies related to rare earth dopants in ZnO films.

This paper deals with optical and electrotransport properties, and defect structure examined by PAS of rare earths doped ZnO thin films prepared by PLD.

## 2. Experimental

ZnO:RE (RE = Sm, Gd, Ho) thin films were grown by PLD (Nd:YAG, $\lambda = 266$ nm, $\tau = 4$ ns, repetition rate = 10 Hz) from $ZnO:Sm_2O_3$, $ZnO:Gd_2O_3$ and $ZnO:Ho_2O_3$ targets (RE content was 1 at.%) in oxygen ambient at pressure of 10 Pa at room temperature. A constant number of shots of 12,000 and laser fluence of 2 J/cm$^2$ were set for each sample deposition. The films were deposited on fused silica (FS) and Si(100) substrates. The distance between the target and the substrate was kept at 45 mm.

The crystal structure and morphology of the films were characterized by X-ray diffraction (XRD, X'Pert, Co $K_\alpha$ radiation, $\lambda = 1.789$ Å) and atomic force microscopy (AFM). The optical properties were analyzed by UV-VIS-NIR spectrophotometry, spectral ellipsometry (SE) (J.A.Woolam M-2000 ellipsometer) and photoluminescence (PL) (He–Cd excitation laser, $\lambda = 325$ nm). The electrotransport properties of samples deposited on FS substrate were analyzed by the van der Pauw method. Gold contacts were pre-sputtered on the FS substrates.

———————

*corresponding author; e-mail: novotnym@fzu.cz

Parameters of ZnO:RE films.

| ZnO:RE sample | Ionic radius RE$^{3+}$ (Ref. [18]) [pm] | Thickness [nm] | Resistivity $\rho$ [$10^4$ $\Omega$ cm] | Band gap [eV] | Positron diffusion length $L_+$ [nm] | $S$ param. | $W$ param. | Mean crystallite size [nm] | Microstrain [%] | Roughness RMS [nm] |
|---|---|---|---|---|---|---|---|---|---|---|
| ZnO:Sm | 95.8 | 195 | 4.26 | 3.32 | 5.9(4) | 0.5318(2) | 0.0937(2) | 40 | 0.098 | 8.1 |
| ZnO:Gd | 93.8 | 194 | 3.44 | 3.26 | 7.3(1) | 0.5294(2) | 0.0948(1) | 50 | 0.129 | 14.1 |
| ZnO:Ho | 90.1 | 213 | 0.0446 | 3.32 | 7.0(2) | 0.5306(2) | 0.0943(2) | 40 | 0.013 | 5.7 |

Variable energy positron annihilation spectroscopy (VEPAS) measurements were performed using a magnetically guided variable energy positron beam SPONSOR in HZDR with positron energies from 30 eV to 30 keV [16]. For each positron energy, the Doppler broadening of the annihilation profile was evaluated using the $S$ and the $W$ parameters. The dependence of the $S$ parameter on positron energy was analyzed using the VEPFIT code [17].

## 3. Results and discussion

The parameters of deposited ZnO:RE films are summarized in Table I. Let us discuss the results of particular analyses and related films properties.

### 3.1. Optical properties

Optical transmission UV–VIS spectra of ZnO:RE films deposited on FS substrate are shown in Fig. 1. The spectra revealed a good optical quality of ZnO material since the average transmittance exceeded 80% in the visible region. Tauc's plot method was used to estimate $E_g$ from a linear extrapolation of the dependence of $(h\upsilon\alpha)^2$ on the photon energy $h\upsilon$ ($\alpha$ is absorption coefficient). We derived $E_g = 3.32$ eV for ZnO:Sm, Ho and $E_g = 3.26$ eV for ZnO:Gd film. The obtained $E_g$ values are in agreement with ZnO:Eu film deposited by PLD [8].

The optical constants of ZnO:RE films deposited on Si substrate extracted from spectral ellipsometry measurement are depicted in Fig. 2. The ellipsometry data were fitted using a multilayer model consisting of Si substrate, native silicon oxide, ZnO:RE, and effective medium approximation (EMA) roughness. ZnO:RE layer was modeled using the Cody–Lorentz and two Gaussian oscillators [19]. The optical constants did not differ compared to undoped ZnO [20].

Photoluminescence emission spectra of ZnO:RE films are shown in Fig. 3. Spectra exhibited typical features of PLD-grown ZnO where a dominating broad deep level emission (DLE) green-yellow band centered around 570 nm and near band edge (NBE) ZnO emission located at 382 nm are present. The defect-related luminescence is due to radiative transitions between deep acceptor (Zn vacancy $V_{Zn}$) and shallow donors (O vacancy $V_O$ and Zn interstitial $Zn_i$) [13]. NBE originated from the free exciton recombination and its longitudinal-optical phonon replica [21]. In case of ZnO:Sm the sharp emission lines
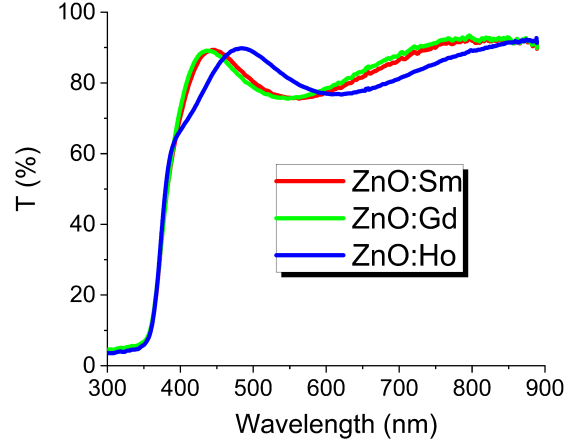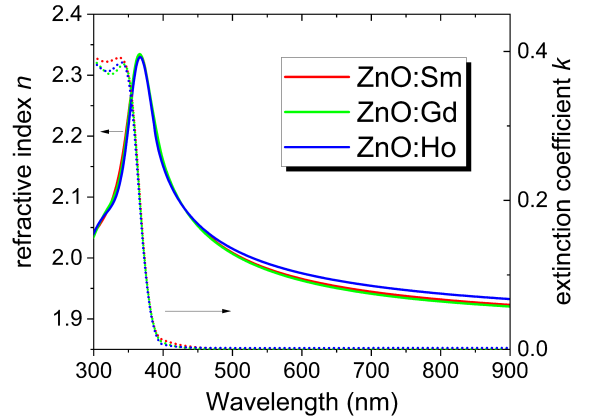


Fig. 1. Optical transmission of ZnO:RE films.



Fig. 2. Optical constants of ZnO:RE films.

superimposed on DLE band positioned at 567, 607, and 658 nm appeared. The lines can be attributed to $^4G_{5/2}-$ $^6H_J$ ($J = 5/2$, 7/2, 9/2) intra-4f transition in $Sm^{3+}$ ions. The appearance of several lines from the $^4G_{5/2}-^6H_J$ transitions suggested the local structure around $Sm^{3+}$ may be inhomogeneous [22]. The energy transfer from ZnO to $Sm^{3+}$ had to take place since $Sm^{3+}$ emission was stimulated by indirect excitation. The $I_{NBE}/I_{DLE}$ ratio of NBE and DLE bands, usually related to the structural imperfection including stoichiometry of the epitaxial ZnO layers, was the highest for ZnO:Sm film ($I_{NBE}/I_{DLE} = 0.155$) while half of that value was obtained for ZnO:Gd, ZnO:Ho films.

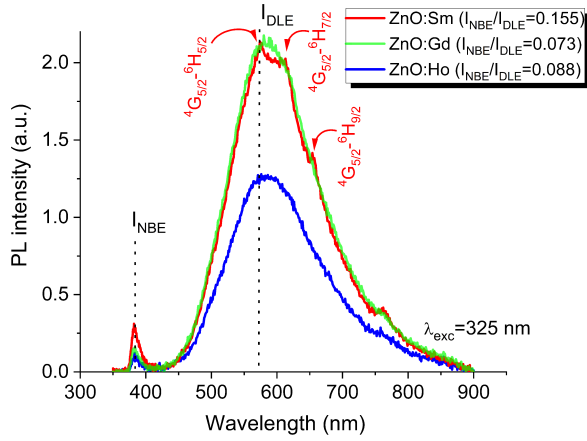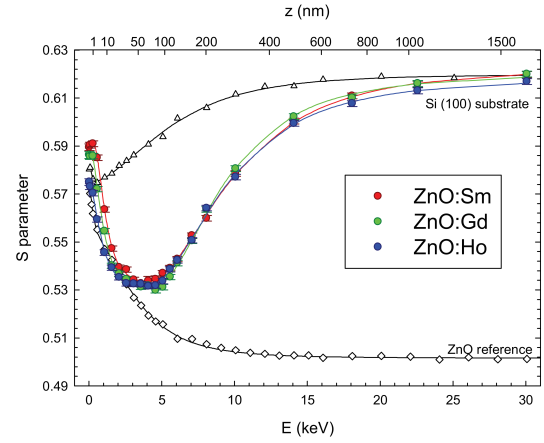Fig. 3. Photoluminescence emission spectra of ZnO:RE films.



Fig. 4. $S(E)$ curves of ZnO:RE films. Solid lines correspond to result of two-layer VEPFIT model. Reference data for zinc oxide monocrystal and Si substrate are included.

In case of ZnO:Gd we did not observe any strong emissions reported around 397, 432, 483, and 514 nm that were supposed to be induced by the impurity levels of Gd introduced into the band gap of the ZnO nanocrystals [4].

### 3.2. Electrotransport properties

The ZnO:Ho sample exhibited substantial lower electrical resistivity $\rho = 4.46 \times 10^2$ $\Omega$ cm compared to ZnO:Gd and ZnO:Sm where $\rho = 4.46 \times 10^4$ $\Omega$ cm and $\rho = 3.44 \times 10^4$ $\Omega$ cm were measured, respectively. The low $\rho$ might be related to lowest microstrain and roughness of ZnO:Ho sample that lead to lower electron scattering. Generally, higher values of $\rho$ are rather characteristic for high quality undoped ZnO prepared by PLD [23, 24], where it seems that Sm and Gd dopant level of 1 at.% does not significantly contribute to PLD-grown ZnO electrical conductivity.

### 3.3. Positron annihilation results

Figure 4 shows dependence of the $S$ parameter of each ZnO:RE film deposited on Si substrate on energy of incident positrons ($S(E)$ curve). At low positron energies ($< 0.5$ keV) virtually all positrons annihilated at the ZnO:RE surface. Higher values of the $S$ parameter for ZnO:Sm and ZnO:Gd films correlated with higher surface roughness determined by AFM (Table I). With increasing energy, the fraction of positrons diffusing from ZnO:RE layer back to the surface gradually decreases as reflected by the decrease of the $S$ parameter. In the energy range from 2 keV to 5 keV almost all positrons annihilated in ZnO:RE film and the $S$ parameter reaches a plateau. One can see in Fig. 4 that the plateau value is substantially higher than the reference value of hydrothermally grown ZnO monocrystal. At higher energies ($> 5$ keV) positrons start to penetrate to the Si substrate and the $S$ parameter increases and eventually at energies above 25 keV reaches constant value close to the Si reference as it is depicted in Fig. 4.

Each $S(E)$ curve was fitted using the two-layer VEPFIT model (ZnO layer and Si substrate).

ZnO:RE films are characterized by their $S$ and $W$ parameter and positron diffusion length $L_+$, which are listed in Table I. In general, thin films prepared by PLD might contain 2 types of defects: (A) vacancy-like open-volume defects associated with grain boundaries or misfit dislocations; (B) intra-granular defects, e.g., Zn and O vacancies. Type A defects characterize the film microstructure, while type B has a strong impact on electrical and optical properties. Considering nanocrystalline character of ZnO:RE films dominating type of defects are supposed to be open volumes associated with the grain boundaries. $L_+$ correlates well with the mean crystallite size determined from XRD.

Since the deposition conditions were kept constant for all ZnO:RE films we might expect formation of the same amount of oxygen and zinc vacancies and examine the sole role of RE dopant. For positron annihilations inside the grains, the $S$ parameter should provide better insight into the dependence on dopant type. $RE^{3+}$ are suggested to substitute $Zn^{2+}$ sites [4], which may lead to local tensile lattice strain due to the smaller ionic radius of $Zn^{2+}$ of 74 pm [18]. Despite different ionic radii of $RE^{3+}$ we observed no significant difference in $S$ parameter. Therefore, from this point of view (defects sensitive to this technique) we can conclude that the defect structure inside the grains is similar for all types of RE. Note that for the $W$ parameter, which is more suitable for resolving different RE types from each other, we did not observe any significant difference either.

## 4. Conclusion

Rare earths (Sm, Gd, Ho) doped ZnO nanocrystalline thin films were grown by PLD at room temperature. The ZnO:RE films exhibited a good optical quality in the

visible spectral region with optical constants similar to undoped ZnO. Photoluminescence spectra of samples revealed typical features of PLD ZnO films — broad deep level emission green-yellow band centered around 570 nm and near band edge ZnO emission located at 382 nm. The intensity ratio of these bands suggested the best quality of ZnO:Sm film where also characteristic emission lines of intra-4f transition of $Sm^{3+}$ ions induced by indirect excitation appeared in the spectra. The spectra indicated the inhomogeneous local structure. The lowest electrical resistivity of $4.46 \times 10^2$ Ω cm together with the lowest microstrain of 0.013% and roughness of 5.7 nm was obtained at ZnO:Ho film.

ZnO:RE thin films contained two types of defects: (A) inter-granular structural defects (grain boundaries); (B) intra-granular defects with a strong impact on electrical and optical properties. The measurement of the $S$ parameter did not reveal any substantial dependence on the type of dopant.

## Acknowledgments

## References

[1] U. Özgür, Y.I. Alivov, C. Liu, A. Teke, M.A. Reshchikov, S. Doğan, V. Avrutin, S.J. Cho, H. Morkoç, *J. Appl. Phys.* **98**, 041301 (2005).

[2] F. Rahman, *Opt. Eng.* **58**, 1 (2019).

[3] L. Chen, J. Zhang, X. Zhang, F. Liu, X. Wang, *Opt. Express* **16**, 11795 (2008).

[4] D. Daksh, Y.K. Agrawal, *Rev. Nanosci. Nanotechnol.* **5**, 1 (2016).

[5] A. Ziani, A. Tempez, C. Frilay, C. Davesnne, C. Labbe, P. Marie, S. Legendre, X. Portier, *Phys. Status Solidi C* **11**, 1497 (2014).

[6] W.M. Jadwisienczak, H.J. Lozykowski, A. Xu, B. Patel, *J. Electron. Mater.* **31**, 776 (2002).

[7] S. Bachir, K. Azuma, J. Kossanyi, P. Valat, J.C. Ronfard-Haret, *J. Lumin.* **75**, 35 (1997).

[8] M. Novotny, M. Vondracek, E. Maresova, et al., *Appl. Surf. Sci.* **476**, 271 (2019).

[9] M. Novotny, E. Maresova, P. Fitl, et al., *Appl. Phys. A* **122**, (2016).

[10] S. Choopun, R.D. Vispute, W. Noch, A. Balsamo, R.P. Sharma, T. Venkatesan, A. Iliadis, D.C. Look, *Appl. Phys. Lett.* **75**, 3947 (1999).

[11] M. Novotny, J. Cizek, R. Kuzel, J. Bulir, J. Lancok, J. Connolly, E. McCarthy, S. Krishnamurthy, J.P. Mosnier, W. Anwand, G. Brauer, *J. Phys. D Appl. Phys.* **45**, (2012).

[12] F. Tuomisto, I. Makkonen, *Rev. Mod. Phys.* **85**, 1583 (2013).

[13] J. Cizek, J. Valenta, P. Hruska, O. Melikhova, I. Prochazka, M. Novotny, J. Bulir, *Appl. Phys. Lett.* **106**, (2015).

[14] O. Melikhova, J. Cizek, I. Prochazka, et al., *J. Phys. Conf. Ser.* **443**, 012018 (2013).

[15] M. Vlcek, J. Cizek, I. Prochazka, M. Novotny, J. Bulir, J. Lancok, W. Anwand, G. Brauer, J.P. Mosnier, *J. Phys. Conf. Ser.* **505**, 012021 (2014).

[16] W. Anwand, G. Brauer, M. Butterling, H.R. Kissener, A. Wagner, *Def. Diff. Forum* **331**, 25 (2012).

[17] A. van Veen, H. Schut, M. Clement, J.M.M. de Nijs, A. Kruseman, M.R. Ijpma, *Appl. Surf. Sci.* **85**, 216 (1995).

[18] R. Shannon, *Acta Crystallogr. A* **32**, 751 (1976).

[19] CompleteEASE, Data Analysis Manual Version 4.63, Woollam, Lincoln (NE) 2011.

[20] Y.C. Liu, J.H. Hsieh, S.K. Tung, *Thin Solid Films* **510**, 32 (2006).

[21] C. Chen, H. He, Y. Lu, K. Wu, Z. Ye, *ACS Appl. Mater. Interfaces* **5**, 6354 (2013).

[22] T. Tsuji, Y. Terai, M.H.B. Kamarudin, M. Kawabata, Y. Fujiwara, *J. Non-Cryst. Solids* **358**, 2443 (2012).

[23] J.N. Zeng, J.K. Low, Z.M. Ren, T. Liew, Y.F. Lu, *Appl. Surf. Sci.* **197**, 362 (2002).

[24] S.P. Heluani, G. Braunstein, M. Villafuerte, G. Simonelli, S. Duhalde, *Thin Solid Films* **515**, 2379 (2006).